HIGHLIGHT

Can metal–nitrogen–carbon catalysts satisfy oxygen electrochemistry?

Cheng Tang and Qiang Zhang*

Transition metal–nitrogen–carbon catalysts have been well-established as the most promising alternatives for oxygen reduction reaction catalysis. The theoretical and atomic-level investigation of their working active sites, insights into their durability, mechanism and bifunctional nature for oxygen electrocatalysis yield further advances aiming at optimizing transition metal–nitrogen–carbon materials for oxygen electrochemistry.

Oxygen electrochemistry, including oxygen reduction reaction (ORR) and oxygen evolution reaction (OER), is a vital cornerstone for various next-generation energy conversion and storage technologies, aiming at sustainable development and mobile technology.[1] Water splitting (OER at the anode of an electrolyzer) and fuel cells (ORR at the cathode)[2–6] contribute to the clean "hydrogen economy", which can be employed in electric vehicles and large-scale applications. Rechargeable metal–air batteries (ORR during discharging and OER during charging at the cathode),[7–10] such as Li–air and Zn–air batteries, are under intense scrutiny owing to their extremely high energy densities. Nevertheless, these multi-step and heterogeneous catalytic processes suffer from sluggish kinetics and pronounced overpotential, leading to a poor energy efficiency which is a bottleneck towards practical applications. Therefore, the rational design of superb catalysts with earth-abundance, superior reactivity, and sufficient stability under operating conditions, preferably which are also bifunctional catalysts for both ORR and OER, is of urgent importance for the development of oxygen electrochemistry-involved devices.[7–12]

Among various candidates, transition metal–nitrogen–carbon (MeNC) catalysts have attracted the most attention and have been regarded as the most promising alternatives for ORR since the pioneering works by Jasinski[13] and Yeager.[14] Macrocyclic complexes, such as metallo-phthalocyanines,[13] were firstly employed as starting materials, and then the pyrolysis of separated metal/carbon/nitrogen precursors (such as polyacrylonitrile,[14] polypyrrole,[15] phenanthroline,[16] polyaniline,[17] and NH$_3$ (ref. 18)), was also demonstrated to be effective but more economical. Historically, the common active sites are supposed to be the metal–nitrogen–carbon moieties (MeN$_x$C, Me = Co, Fe, Ni, Mn, *etc.*, and normally $x = 2$ or 4), with metal cations being coordinated by pyridinic/pyrrolic nitrogen

functionalities in the center or edge of a graphitic matrix (Fig. 1a).[19,20] It was indicated that the formation of Me–N$_4$ clusters was more energetically feasible at the edges of a graphitic pore, and Co/Fe-based MeNC electrocatalysts were predicted to be more active than Ni-based MeNC catalysts.[21] Besides, the activity is also greatly influenced by the nanocarbon structures[22–25] and bimetallic composites can demonstrate a synergetic effect towards enhanced performances.[26,27] The interaction between d-electrons of metal ions and π-electrons in the carbon basal plane can modify the local electronic structure, leading to a favourable adsorption of intermediates and a higher activity.[28] This has been widely supported by various characterizations, such as X-ray photoelectron spectroscopy,[29,30] extended X-ray absorption fine structure (EXAFS),[29,31,32] X-ray
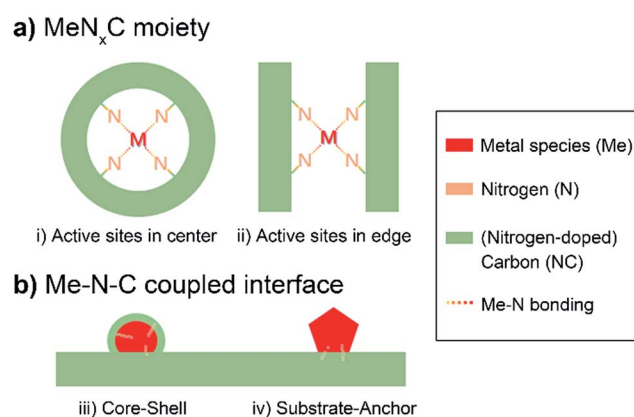

Fig. 1 Schematic representation of two kinds of MeNC catalysts: (a) MeN$_x$C moieties, such as (i) porphyrin-like, or phthalocyanine-like macrocyclic complexes with active sites in the center, and (ii) active sites at the edge, bridging separate sections of NC sheets; (b) Me–N–C coupled interface, including the (iii) core–shell structure with a metal/metal carbide/metal oxide core and NC shell, and (iv) substrate-anchor structure with a metal-containing particle strongly coupled on the NC surface.

Beijing Key Laboratory of Green Chemical Reaction Engineering and Technology, Department of Chemical Engineering, Tsinghua University, Beijing 100084, China. E-mail: zhang-qiang@mails.tsinghua.edu.cn

4998 | *J. Mater. Chem. A*, 2016, **4**, 4998–5001

This journal is © The Royal Society of Chemistry 2016

absorption near-edge spectra (XANES),[29,31,32] Mössbauer spectroscopy,[23,32–34] electron microscopy imaging coupled with electron energy loss spectra,[31] and density functional theory computation.[21,28,32,35]

In practice, high-temperature treatment is always conducted to improve the durability, whereas, the atomic configuration of MeN_xC tends to decompose and transfer to metal/metal oxide/metal carbide–nitrogen–carbon structures (Me–N–C), in which case the activity is ascribed to the strongly coupled interface (Fig. 1b). The resultant substrate-anchor configuration endows a synergetic host–guest electronic interaction and additionally the core–shell structure exhibits a protective graphitic shell, thereby leading to a considerably improved activity and stability.[26,27,36–47] In spite of the intensive investigation and extraordinary performances of MeNC catalysts in both acidic and alkaline conditions, the characterization of working active sites and underlying governances are still indistinct. What's more, the fundamental understanding of the mechanism of instability, specifically under operating conditions, is hitherto rarely reported.

Encouragingly, in a very recent report, Zitolo *et al.* reported the systematic identification of active sites in Fe–N–C catalysts for ORR in acid.[32] Assisted by the quantitative analysis of EXAFS and XANES results both experimentally and theoretically, they elucidated the porphyrin-like FeN_4C_{12} moieties as real active sites for Fe–N–C materials ((i) in Fig. 2a). These structures were expected to be generated in disordered graphene sheets or micropores bridging zigzag graphene edges. Additionally,

a higher basic property of the N-carbon support due to NH_3 pyrolysis was demonstrated to be critical for the activity enhancement of ORR catalysis. This work provides atomic-scale knowledge of the real active sites and the site-support interactions, thereby promoting the bottom-up synthesis of advanced MeNC catalysts. Recently, Bao and co-workers have successfully revealed the atomic structure of FeN_4 sites in graphene by a comprehensive implementation of advanced microscopy techniques ((ii) in Fig. 2a),[48] as a strong and visual support for the spectrum analysis.[32]

Besides the origin of activity, insights into the durability mechanism are more important for practical applications. Recently, Mayrhofer *et al.* implemented systematic electrochemical characterizations coupled with advanced online and *operando* analytical techniques to investigate the degradation mechanism of a model Fe–N–C catalyst in acid (Fig. 2b).[49] The Fe appeared dominantly as FeN_xC moieties (91%), with minor metallic Fe or iron oxide/carbide present. With the online scanning flow cell/inductively coupled plasma mass spectrometry system, direct demetalation of Fe from Fe-based crystalline structures was observed at low potential (<0.7 V_{RHE}, RHE = reversible hydrogen electrode). Although the Fe dissolution might potentially induce damage to polymer electrolyte membrane fuel cell systems, such as partial exchange of protons and generation of radical oxygen species, it did not induce significant ORR activity decay as the leached crystalline structures were poorly active, while the solvated Fe^{2+} cations in the active FeN_xC moieties were stable at $E < 0.77$ V_{SHE} (SHE = standard hydrogen electrode)
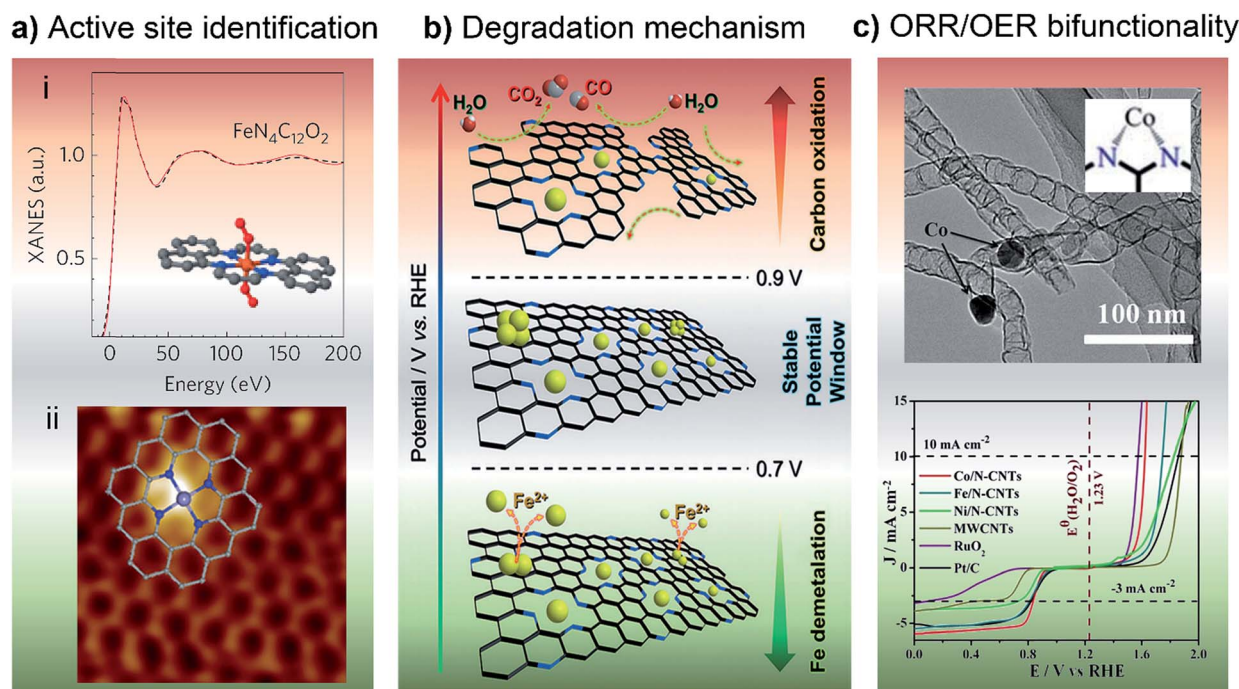

Fig. 2 Characterization and mechanistic investigation of MeNC catalysts. (a) Active site identification: (i) comparison of the experimental and theoretical K-edge XANES spectra for FeN_4C_{12} with two O_2 molecules adsorbed in the side-on mode.[32] (ii) Low-temperature scanning tunneling microscopy image of FeN_4 center in graphene.[48] (b) Schematic illustration of the degradation mechanism of Fe–N–C catalysts for ORR. The Fe demetalation is observed in the low potential region (<0.7 V), while carbon tends to be oxidized in the higher potential region (>0.9 V), leading to a stable potential window (0.7–0.9 V).[49] (c) ORR/OER bifunctionality of MeNC catalysts (Me = Co, Fe, and Ni).[50]

This journal is © The Royal Society of Chemistry 2016

J. Mater. Chem. A, 2016, **4**, 4998–5001 | **4999**

in acid medium. Contrastively, the carbon oxidation in high potential (>0.9 V_{RHE}) regions was found to be primarily responsible for the activity loss. The carbon edges were corroded and led to the indirect leaching of Fe involved in the active FeN_xC structures, thereby resulting in a poor durability. These fresh observations are highly instructive and provide some guidelines towards the rational design and operation optimization of electrocatalysts.

Notably, the potential capability of MeNC configurations for bifunctional ORR and OER catalysts has also been revealed recently by Li and co-workers.[50] They proposed a cost-effective strategy to prepare Fe/Co/Ni encapsulated N-doped carbon nanotube (CNT) hybrids *via* a facile solid-state reaction of cyanamide and metal chloride. As shown in Fig. 2c, the Co/N-CNT catalyst was demonstrated to deliver an excellent bifunctionality towards both ORR and OER in alkaline conditions. The voltage gap between the half-wave potential for ORR and the potential required for a 10 mA cm^{-2} OER current density was as low as 0.78 V. Additionally, Qiao *et al.* elucidated the promising bifunctional catalysis in alkaline conditions based on a free-standing hybrid film with exfoliated Ti_3C_2 and g-C_3N_4 sheets made by layer-by-layer self-assembly.[51] A proof-to-concept test in rechargeable Zn–air batteries implied its stable activity for both ORR and OER. The XPS analysis exhibited a noticeably negative shift (0.9 eV) of Ti–C $2p_{3/2}$ and a split N 1s spectrum for triazine rings (C=N–C), indicating the strong coupling between N in g-C_3N_4 and Ti in Ti_3C_2. Noticeably, the fabrication of such a free-standing and binder-free electrocatalyst as a direct electrode is effective and favorable for long-term operation due to the lower interfacial resistance and potentially diminished polarization.[49]

Taken together, the above-highlighted investigations unravel the atomic-scale active sites, the underlying degradation mechanism for MeNC catalysts in acid or alkaline conditions and even potential bifunctionalities for both ORR and OER. It indicates that this family of materials is a promising solution for oxygen electrochemistry with high activity, superb stability, rich reserves, and facile production. Clearly, some significant issues still need to be addressed to advance this field and satisfy the practical requirements.

Of particular importance will be the identification and optimization of the metallic species, such as the element (Co, Fe, Ni, Mn, Ti, *et al.*), and the structure (coordinated ions, metallic, oxide or carbide particles),[52] aiming at specific catalysis or operating conditions. The nature of the active sites and favorite modes of MeNC configurations deserve intensive and fundamental studies. The activity and durability should be further improved by the nano-engineering of electrocatalysts, integration of cathodes, and design of process. Laboratory-scale, or even pilot-scale demonstrations of MeNC catalysts in integrated fuel cells, metal–air batteries, and water electrolyzers are the next challenges. More advanced, especially *in situ* or *operando* methods are highly expected to be coupled and implemented in this research field for better investigation and developments of these materials. Any breakthrough in the above aspects is believed to be a tremendous contribution to the practical applications of MeNC catalysts, other analogous materials and the corresponding next-generation energy technologies.

Notes and references

1 I. Katsounaros, S. Cherevko, A. R. Zeradjanin and K. J. J. Mayrhofer, *Angew. Chem., Int. Ed.*, 2014, **53**, 102–121.
2 M. K. Debe, *Nature*, 2012, **486**, 43–51.
3 J. Suntivich, H. A. Gasteiger, N. Yabuuchi, H. Nakanishi, J. B. Goodenough and Y. Shao-Horn, *Nat. Chem.*, 2011, **3**, 546–550.
4 Y. Gorlin and T. F. Jaramillo, *J. Am. Chem. Soc.*, 2010, **132**, 13612–13614.
5 Y. Y. Liang, Y. G. Li, H. L. Wang, J. G. Zhou, J. Wang, T. Regier and H. J. Dai, *Nat. Mater.*, 2011, **10**, 780–786.
6 C. Tang, H. S. Wang, H. F. Wang, Q. Zhang, G. L. Tian, J. Q. Nie and F. Wei, *Adv. Mater.*, 2015, **27**, 4516–4522.
7 F. Y. Cheng and J. Chen, *Chem. Soc. Rev.*, 2012, **41**, 2172–2192.
8 Z. Q. Peng, S. A. Freunberger, Y. H. Chen and P. G. Bruce, *Science*, 2012, **337**, 563–566.
9 L. Grande, E. Paillard, J. Hassoun, J. B. Park, Y. J. Lee, Y. K. Sun, S. Passerini and B. Scrosati, *Adv. Mater.*, 2015, **27**, 784–800.
10 Y. G. Li and H. J. Dai, *Chem. Soc. Rev.*, 2014, **43**, 5257–5275.
11 Y. Jiao, Y. Zheng, M. T. Jaroniec and S. Z. Qiao, *Chem. Soc. Rev.*, 2015, **44**, 2060–2086.
12 G. L. Tian, M. Q. Zhao, D. S. Yu, X. Y. Kong, J. Q. Huang, Q. Zhang and F. Wei, *Small*, 2014, **10**, 2251–2259.
13 R. Jasinski, *Nature*, 1964, **201**, 1212–1213.
14 S. Gupta, D. Tryk, I. Bae, W. Aldred and E. Yeager, *J. Appl. Electrochem.*, 1989, **19**, 19–27.
15 R. Bashyam and P. Zelenay, *Nature*, 2006, **443**, 63–66.
16 M. Lefevre, E. Proietti, F. Jaouen and J. P. Dodelet, *Science*, 2009, **324**, 71–74.
17 G. Wu, K. L. More, C. M. Johnston and P. Zelenay, *Science*, 2011, **332**, 443–447.
18 J. H. Zagal, F. Bedioui and J.-P. Dodelet, *N_4-macrocyclic metal complexes*, Springer, New York, 2006.
19 Z. W. Chen, D. Higgins, A. P. Yu, L. Zhang and J. J. Zhang, *Energy Environ. Sci.*, 2011, **4**, 3167–3192.
20 Q. Li, R. G. Cao, J. Cho and G. Wu, *Phys. Chem. Chem. Phys.*, 2014, **16**, 13568–13582.
21 S. Kattel and G. Wang, *J. Mater. Chem. A*, 2013, **1**, 10790–10797.
22 B. Y. Xia, Y. Yan, N. Li, H. B. Wu, X. W. Lou and X. Wang, *Nat. Energy*, 2016, **1**, 15006.
23 S. Zhang, B. Liu and S. Chen, *Phys. Chem. Chem. Phys.*, 2013, **15**, 18482–18490.
24 X. Wang, H. Fu, W. Li, J. Zheng and X. Li, *RSC Adv.*, 2014, **4**, 37779–37785.
25 J. Du, F. Cheng, S. Wang, T. Zhang and J. Chen, *Sci. Rep.*, 2014, **4**, 4386.
26 S. Brueller, H.-W. Liang, U. I. Kramm, J. W. Krumpfer, X. Feng and K. Muellen, *J. Mater. Chem. A*, 2015, **3**, 23799–23808.

27 R. Zhang, S. He, Y. Lu and W. Chen, *J. Mater. Chem. A*, 2015, **3**, 3559–3567.

28 M. H. Seo, D. Higgins, G. Jiang, S. M. Choi, B. Han and Z. Chen, *J. Mater. Chem. A*, 2014, **2**, 19707–19716.

29 J. Masa, W. Xia, I. Sinev, A. Q. Zhao, Z. Y. Sun, S. Grutzke, P. Weide, M. Muhler and W. Schuhmann, *Angew. Chem., Int. Ed.*, 2014, **53**, 8508–8512.

30 H. W. Liang, W. Wei, Z. S. Wu, X. L. Feng and K. Mullen, *J. Am. Chem. Soc.*, 2013, **135**, 16002–16005.

31 J. L. Shui, N. K. Karan, M. Balasubramanian, S. Y. Li and D. J. Liu, *J. Am. Chem. Soc.*, 2012, **134**, 16654–16661.

32 A. Zitolo, V. Goellner, V. Armel, M. T. Sougrati, T. Mineva, L. Stievano, E. Fonda and F. Jaouen, *Nat. Mater.*, 2015, **14**, 937–942.

33 Y. Zhu, B. Zhang, X. Liu, D.-W. Wang and D. S. Su, *Angew. Chem., Int. Ed.*, 2014, **53**, 10673–10677.

34 S. Zhang, H. Zhang, Q. Liu and S. Chen, *J. Mater. Chem. A*, 2013, **1**, 3302–3308.

35 N. Ramaswamy, U. Tylus, Q. Y. Jia and S. Mukerjee, *J. Am. Chem. Soc.*, 2013, **135**, 15443–15449.

36 Z. H. Wen, S. Q. Ci, F. Zhang, X. L. Feng, S. M. Cui, S. Mao, S. L. Luo, Z. He and J. H. Chen, *Adv. Mater.*, 2012, **24**, 1399–1404.

37 Z. S. Wu, L. Chen, J. Z. Liu, K. Parvez, H. W. Liang, J. Shu, H. Sachdev, R. Graf, X. L. Feng and K. Mullen, *Adv. Mater.*, 2014, **26**, 1450–1455.

38 Y. Hu, J. O. Jensen, W. Zhang, L. N. Cleemann, W. Xing, N. J. Bjerrum and Q. F. Li, *Angew. Chem., Int. Ed.*, 2014, **53**, 3675–3679.

39 H. T. Chung, J. H. Won and P. Zelenay, *Nat. Commun.*, 2013, **4**, 1922.

40 H. L. Jiang, Y. F. Yao, Y. H. Zhu, Y. Y. Liu, Y. H. Su, X. L. Yang and C. Z. Li, *ACS Appl. Mater. Interfaces*, 2015, **7**, 21511–21520.

41 H. Jiang, Y. Su, Y. Zhu, J. Shen, X. Yang, Q. Feng and C. Li, *J. Mater. Chem. A*, 2013, **1**, 12074–12081.

42 J. Sanetuntikul, C. Chuaicham, Y.-W. Choi and S. Shanmugam, *J. Mater. Chem. A*, 2015, **3**, 15473–15481.

43 J. Wang, D. Gao, G. Wang, S. Miao, H. Wu, J. Li and X. Bao, *J. Mater. Chem. A*, 2014, **2**, 20067–20074.

44 J. Xu, Q. Yu, C. Wu and L. Guan, *J. Mater. Chem. A*, 2015, **3**, 21647–21654.

45 Y. Yao, H. Xiao, P. Wang, P. Su, Z. Shao and Q. Yang, *J. Mater. Chem. A*, 2014, **2**, 11768–11775.

46 J. Zhang, D. He, H. Su, X. Chen, M. Pan and S. Mu, *J. Mater. Chem. A*, 2014, **2**, 1242–1246.

47 C. Y. Su, B. H. Liu, T. J. Lin, Y. M. Chi, C. C. Kei, K. W. Wang and T. P. Perng, *J. Mater. Chem. A*, 2015, **3**, 18983–18990.

48 D. Deng, X. Chen, L. Yu, X. Wu, Q. Liu, Y. Liu, H. Yang, H. Tian, Y. Hu, P. Du, R. Si, J. Wang, X. Cui, H. Li, J. Xiao, T. Xu, J. Deng, F. Yang, P. N. Duchesne, P. Zhang, J. Zhou, L. Sun, J. Li, X. Pan and X. Bao, *Sci. Adv.*, 2015, **1**, e1500462.

49 C. H. Choi, C. Baldizzone, J. P. Grote, A. K. Schuppert, F. Jaouen and K. J. J. Mayrhofer, *Angew. Chem., Int. Ed.*, 2015, **54**, 12753–12757.

50 Y. Liu, H. Jiang, Y. Zhu, X. Yang and C. Li, *J. Mater. Chem. A*, 2016, **4**, 1694–1701.

51 T. Y. Ma, J. L. Cao, M. Jaroniec and S. Z. Qiao, *Angew. Chem., Int. Ed.*, 2016, **55**, 1138–1142.

52 Y. Zhu, B. Zhang, D.-W. Wang and D. S. Su, *ChemSusChem*, 2015, **8**, 4016–4021.

This journal is © The Royal Society of Chemistry 2016

J. Mater. Chem. A, 2016, **4**, 4998–5001 | **5001**